UCRL-JRNL-229152

LAWRENCE
LIVERMORE
NATIONAL
LABORATORY

Non-destructive Identification of Individual Leukemia Cells by Optical Trapping Raman Spectroscopy

J. W. Chan, D. S. Taylor, S. Lane, T. Zwerdling, J. Tuscano, T. Huser

March 16, 2007

Analytical Chemistry

This document was prepared as an account of work sponsored by an agency of the United States Government. Neither the United States Government nor the University of California nor any of their employees, makes any warranty, express or implied, or assumes any legal liability or responsibility for the accuracy, completeness, or usefulness of any information, apparatus, product, or process disclosed, or represents that its use would not infringe privately owned rights. Reference herein to any specific commercial product, process, or service by trade name, trademark, manufacturer, or otherwise, does not necessarily constitute or imply its endorsement, recommendation, or favoring by the United States Government or the University of California. The views and opinions of authors expressed herein do not necessarily state or reflect those of the United States Government or the University of California, and shall not be used for advertising or product endorsement purposes.

Updated October 14, 2003

Non-destructive Identification of Individual Leukemia Cells by Laser Trapping Raman Spectroscopy

James W. Chan[*,1,2], *Douglas S. Taylor*[2,3], *Stephen M. Lane*[1,2], *Theodore Zwerdling*[2,3],

Joseph Tuscano[4], *Thomas Huser*[2,5]

1. Applied Physics and Biophysics Division, Physical Sciences Directorate, Lawrence Livermore National Laboratory, P.O. Box 808, L-211, Livermore, CA 94551

2. NSF Center for Biophotonics Science and Technology, University of California, Davis, 2700 Stockton Blvd, Suite 1400, Sacramento, CA 95817

3. Department of Pediatrics, Section of Hematology-Oncology, University of California, Davis, 2516 Stockton Blvd, Sacramento, CA 95817

4. Division of Hematology and Oncology, Department of Internal Medicine, University of California, Davis, Sacramento, CA 95817

5. Division of Endocrinology, Clinical Nutrition, and Vascular Medicine, Department of Internal Medicine, University of California, Davis, 4150 V Street, PPSB Suite G400, Sacramento, CA 95817

Running Title : Raman spectroscopy of single leukemia cells

*Corresponding author: James Chan, (925) 423-3565, fax: (925) 424-2778, chan19@llnl.gov

Abstract

Currently, a combination of technologies is typically required to assess the malignancy of cancer cells. These methods often lack the specificity and sensitivity necessary for early, accurate diagnosis. Here we demonstrate using clinical samples the application of laser trapping Raman spectroscopy as a novel approach that provides intrinsic biochemical markers for the noninvasive detection of individual cancer cells. The Raman spectra of live, hematopoietic cells provide reliable molecular fingerprints that reflect their biochemical composition and biology. Populations of normal T and B lymphocytes from four healthy individuals, and cells from three leukemia patients were analyzed, and multiple intrinsic Raman markers associated with DNA and protein vibrational modes have been identified that exhibit excellent discriminating power for cancer cell identification. A combination of two multivariate statistical methods, principal component analysis (PCA) and linear discriminant analysis (LDA), was used to confirm the significance of these markers for identifying cancer cells and classifying the data. The results indicate that, on average, 95% of the normal cells and 90% of the patient cells were accurately classified into their respective cell types. We also provide evidence that these markers are unique to cancer cells and not purely a function of differences in their cellular activation.

KEYWORDS

Raman spectroscopy, laser tweezers, leukemia, single cell, label-free

INTRODUCTION

Raman spectroscopy, which analyzes molecular bond vibrations by the inelastic scattering of photons, has developed over the past several years into a technique capable of assessing malignancy of cancer tissues during surgery (1). The strengths of this technique are its high sensitivity and chemical specificity without the need for optical labels (H&E stains, fluorescent probes), instead relying on Raman spectral markers of intrinsic biochemical components. Whereas results of histochemical stains are subject both to variability of preparative techniques in the laboratory and subjective interpretation, Raman analysis provides a more objective means of analysis, making it well suited to determine tumor margins during surgery or analyzing pre-cancerous tissues in the esophagus, colon, and cervix (2-5).

Raman studies on cancer detection have predominantly focused on analyzing tissue sections. A single cell approach would improve the sensitivity needed for cancer detection, since a major limitation of bulk Raman analysis is the difficulty in detecting the Raman signals from a small population of cancer cells when masked by stronger signals from the majority of neighboring healthy cells. Optical trapping in combination with confocal Raman spectroscopy has been shown to be a useful method for single cell analysis in solution (6-11), but its application to cancer research has thus far been limited (12,13). In this method, a single, tightly focused laser beam functions as both the laser tweezers to immobilize a freely diffusing cell and the excitation source for generating Raman spectra of the trapped cell. Optical trapping Raman spectroscopy is a novel method for the potential identification and sorting of living cells based on intrinsic Raman signatures in an aqueous flow or static environment. Furthermore, interrogation using Raman spectroscopy minimally disturbs the native state of cells under analysis. Therefore, the cells, which do not require fixing or tagging with otherwise toxic fluorescent dyes, can be subjected to further analysis. In addition, the noninvasiveness of this method makes it an attractive tool for monitoring dynamic cellular processes at the single cell level (14-18), which is useful for assessing response to treatment.

Here, we show that the favorable properties of Raman spectroscopy are maintained even at the single cell level, which offers significant potential for the label-free analysis of individual cancer cells. We

have previously demonstrated that this method can discriminate between normal lymphocytes and transformed Jurkat T and Raji B cultured cell lines (12). The present report significantly extends this analysis to clinical patient samples, where we identify characteristic Raman spectral features associated with DNA, RNA, and protein molecular vibrations for discriminating patient-derived leukemia cells from normal human lymphocytes. We also investigate the spectral changes associated with metabolic activity of normal cells and their effect on the ability to accurately identify cancer cells. Using multivariate statistical methods for interpretation and classification of the Raman data, we demonstrate the robustness, sensitivity, and reproducibility of single cell laser tweezers Raman spectroscopy to acquire Raman fingerprints of individual cells for discriminating between healthy and cancerous cells. Laser trapping Raman technology, optical cancer markers, and statistical techniques are important components in the development of Raman-based diagnostic tools that will be applicable to many areas of biomedical research.

EXPERIMENTAL SECTION

Cell preparation

Normal human peripheral blood mononuclear cells (PBMC) and leukemia cells were obtained by Ficoll-Hypaque density gradient of heparinized venous blood obtained from healthy volunteers or patients with leukemia, respectively. The cells were washed 3 times in RPMI 1640 medium prior to purification. Normal T-cells were separated by rosette formation with activated sheep red blood cells followed by Ficoll-Hypaque density gradient centrifugation. The lymphocytes in the B-enriched fraction are routinely greater than 95% surface immunoglobulin positive as assessed by flow cytometry. T-cells were recovered from the rosetted pellet after twice lysing the sheep red blood cells with ammonium chloride buffer and thrice washing with RPMI 1640 medium. Both T- and B-cell populations were suspended in RPMI 1640 medium supplemented with 10% fetal calf serum at a density of approximately 10^6 cells/ml. T- and B-lymphocytes were stimulated for 18 hours prior to analysis with phytohemagglutinin (10 mcg/ml) or anti-human IgM (5 mcg/ml), respectively. All cell preparations were >99% viable as assessed by trypan blue dye exclusion. Immediately prior to Raman spectra

analysis the cells were washed and suspended in phosphate buffered saline (PBS). The use of fresh human samples for this study was in accordance with the University of California Institutional Review Board practice guidelines.

Laser tweezers Raman spectroscopy

The experimental setup combines an inverted confocal microscope with a single 633 nm wavelength helium-neon laser that functions as both the excitation laser for Raman spectroscopy and as a single Gaussian beam optical trap. The 6 mm diameter laser beam is directed into a 100x, 1.3 NA oil immersion objective and focused through a microscope coverslip on which a solution of cells is placed. The laser power before the objective is roughly 10 mW, resulting in a power density at the focus of approximately 1.3 x 10^9 mW/cm^2. Raman signals generated from the trapped cell are epi-detected, focused through a 100 micron pinhole, and directed toward a spectrometer equipped with a liquid nitrogen cooled, back-thinned, CCD camera. A holographic notch filter is used in the detection arm of the setup to remove residual Rayleigh scattered 633 nm light from entering the spectrometer. Integration times for acquiring a Raman spectrum of a cell are typically 2 to 3 minutes.

Data Processing

A MATLAB routine was written for the purpose of background subtraction and normalization of the data. Each Raman spectrum was background subtracted using an automated routine previously described by Lieber et. al. (19). The intensity of each spectrum was normalized to the 1450 cm^{-1} peak to enable direct comparison of the data.

Multivariate statistical analysis of the data

Each Raman spectrum consists of 1340 channels, but only a fraction of the channels contains useful information for cell classification. Principal component analysis (PCA) (20) is performed on the data set with the goal of defining a new dimensional space in which the major variance in the original data set can be captured and represented by only a few principal component (PC) variables and allowing the most important channels responsible for these differences to be identified. In this analysis, background subtracted and normalized Raman spectra from different cell groups are chosen for comparison and implemented into a PCA MATLAB routine. The program delivers values of the PCs as well as the

loading values for each of the PCs, which provides information on the relative importance of each of the original Raman channels for maximizing the data variance. The PC values are then subjected to linear discriminant analysis (LDA), a method that maximizes between-group and minimizes within-group separation for optimizing data classification. For data classification, we also used a five-fold cross validation method to determine the sensitivity of Raman spectroscopy for cancer detection. In this approach, the data are randomly divided into five different groups, with one group treated as the blind sample and the remaining four used as the training set to define the principal component axes. This process was then repeated for each group until all samples were classified. Performing the classification in this manner is ideal for data sets with limited number of samples, and ensures that the data to be classified does not bias the algorithm.

RESULTS AND DISCUSSION

Hematopoietic cells from healthy individuals exhibit reproducible Raman spectra

The Raman spectra of normal, living T and B lymphocytes obtained from different healthy human subjects were characterized to assess the reproducibility of their signatures from cell-to-cell and from person-to-person. Figure 1 shows the Raman spectra of T and B cells from four volunteers, where each spectrum is an average of 10 to 20 cells. The spectral intensities are normalized to the 1450 cm^{-1} peak to allow for direct comparison of the different Raman spectra. All spectra exhibit similar overall features, and are characterized by Raman peaks corresponding to specific DNA backbone, DNA ring bases, proteins, and amino acid vibrations that have been previously assigned (12,21). The most prominent spectral peaks associated with DNA vibrations were chosen for comparison of their average values and standard deviations for each of the cell groups. Figure 2 shows the results of this comparison for the 785, 1093, 1373, and 1575 cm^{-1} Raman peaks. Next, principal component analysis (PCA) was performed on the data set to determine the variability between cells and between individuals when taking into account contributions from all of the Raman channels. Figure 3 shows the PCA scatter plots using the first two principal components, which account for ~40% of the total variance. For both cell types, the data points cluster together in a small region within the plots. Linear discriminant analysis (LDA) (20) performed on the principal component scores showed that, on average, only a small

percentage of the cells (42% and 48% of the T and B cells respectively) could be correctly classified to each particular individual.

These results show that the Raman spectra of normal T and B cells are highly reproducible both at the cellular level and also between individuals. This is reflected both in the statistical results of select Raman peaks (Figure 2), which show minimal differences in their average intensity values and high p-values relative to a significance level of 0.01, and the PCA plots (Figure 3), which show that the cell clusters all overlap and cannot be distinguished by any clear delineation between different groups. In addition, the low 42% and 48% sensitivity values from the LDA analysis indicate the low variability in the T and B cell Raman spectra from individual to individual and therefore the difficulty in accurately identifying cells from specific individuals. This suggests the feasibility of using the spectra as highly reproducible, universal fingerprints of these cell phenotypes. Furthermore, and most important for this current work, the variations among individual cells as observed here are small when compared to their differences to the cancer cells (discussed below), which shows the ability to discriminate normal and cancer cells from different individuals.

Leukemic cells from clinical samples are distinguishable from normal cells

Leukemia cells were obtained from the peripheral blood of three patients, two diagnosed with pre-B cell leukemia and one with T-cell leukemia. 98%, 81%, and 80% of their lymphocytes were classified as leukemic cells, respectively, based on standard flow cytometry analysis using a combination of light scattering and fluorescence immunolabeling. Thirty to fifty cells of each cell type were probed individually to obtain their Raman spectra. Figure 4 illustrates the mean Raman spectra of the leukemic cells. These spectra are directly compared to the spectra of normal cells to identify the most significant spectral differences. For simplicity, the normal T and B cells from one of the healthy individuals is used in this comparison. Also shown are the difference spectra, obtained by subtracting the normal cell spectra from their corresponding leukemia cell spectra. Consistent spectral differences between the normal and leukemia cell spectra can be seen for all three cases. These differences include changes in the Raman peak intensities located at 678, 785, 1093, 1126, 1337, 1373, 1447, 1575, 1605, 1615, and 1650 cm^{-1}. A consistent slight shift in the 1003 cm^{-1} vibration is also observed in all three cases. Mean

values and standard deviation values for select DNA peaks that differ between normal and cancer cells are plotted in Figure 5 to show the magnitude of the variations. The results of PCA performed on the data sets are shown in Figure 6, in which the cancer cells are compared to a set of healthy cells. Cancer and normal cells form distinct, separate groups in all three cases. The first PC accounts for ~50% of the total variance in the data and is a significant component for differentiating cancer and normal cells.

Table 1 lists the most significant Raman spectral differences between the normal and leukemia cells, as shown in the difference spectra (Figures 4a-4c). Several peaks that are distinct to nucleic acid molecular vibrations, such as the 678, 785, 1337, 1373, 1485, 1510, and 1575 cm^{-1} ring breathing modes, are noticeably weaker in intensity for the neoplastic cells, indicating that the overall nucleic acid content (or nucleic acid to protein ratio) in the probe volume defined by the focused laser beam is lower in neoplastic cells than in normal cells. The neoplastic cell spectra also exhibit a similar reduction in intensity of the 1093 cm^{-1} peak, which is assigned to the symmetric PO^{2-} stretching vibration of the DNA backbone. This further confirms the reduction in nucleic acid content. In contrast, many peaks associated with protein vibrations increase in intensity in the T- and pre-B leukemia cell spectra, indicating a locally higher protein concentration in these cells. These peaks include the 1126 cm^{-1} C-N stretching vibration, the 1605 and 1615 cm^{-1} C=C vibrations, and the 1650 cm^{-1} amide I vibration. In general, most of the differences presented in this study are consistent with those reported in our previous work (12) in which we compared the Raman spectra of normal T and B cells to transformed Jurkat T and Raji B cells. It should be noted that the magnitude of the changes observed for the patient cells, however, appear less pronounced than for the transformed T and B cell lines.

Comparison of the mean intensities of several select peaks in Figure 5 and calculation of the p-values confirm that the differences between the normal and cancer cell spectra are significantly different in all three comparisons, given a 0.01 significance level criterion. These differences are more pronounced than the differences between normal cells from multiple individuals, as was shown in Figure 2. Rather than analyze each Raman wavenumber channel independently, PCA is used to compare the entire spectrum of all the cells simultaneously. PCA plots comparing the normal cells to the three different leukemia cell samples show a clear demarcation between the different cell groups. The significant

Raman channels that are responsible for the separation of the data groups can be extracted by analyzing the loading values that contribute to the principal components, with those channels showing the largest deviations from a zero baseline being the most significant. Figure 7 shows the loading values for the first PC from each of the comparisons in Figure 4. Their similarity to the difference spectra indicates that the spectral features used to discriminate between normal and cancer cells in the PCA are, indeed, associated with the Raman markers discussed earlier.

The first two PCs, which account for close to 70% of the variance, were used in a linear discriminant analysis (LDA) routine to determine the sensitivity of this novel single cell characterization technique. Optical trapping Raman spectroscopy was able to accurately classify the cells for all three cases. The sensitivity values are 95.6% for normal T cells and 88.9% for T-cell leukemia, 91.7% for normal B cells and 93.5% for pre B-cell leukemia, as well as 97.1% for normal B cells and 86.8% for pre B-cell leukemia when we evaluate all three patient samples separately against the normal cells. These sensitivity levels compare very favorably to the flow cytometry results presented earlier.

Overall, the spectra are highly reproducible from cell-to-cell within a particular cell group. This has been observed previously in the analysis of cultured cells (12). We attribute the homogeneity of the spectral signals to the fact that we are consistently probing the nucleus of the individual cells. All of the cells in this study were of a size (~10 μm in diameter) that enabled them to be optically trapped in solution. Since lymphocytes have a relatively large nucleus-to-cytoplasm ratio, there is a high probability that the nucleus is consistently trapped and analyzed within the focal volume, which would explain the consistent presence of very prominent DNA spectral signatures in all of the acquired Raman spectra. This point will be discussed in greater detail in a forthcoming publication. Also, tumbling of the cell within the laser trap for the duration of the time that the cell is being probed will likely result in some spatial averaging of the Raman signals. It should also be noted that trapping of a cell for several minutes did not change the Raman spectra, providing evidence that cells are not being altered by the laser beam.

Elucidating the biology associated with the Raman spectral differences

To determine the biological significance of the spectral differences observed between normal and transformed leukemia/cancer cells, additional experiments were performed to characterize the Raman signatures of activated, non-cancerous T and B cells for direct comparison to the leukemia cell spectra. Whereas most (>95%) of the non-cancerous, unstimulated T- and B- cells are expected to be resting or unstimulated in the G0 phase of cell cycle, a larger fraction of the leukemic cells is expected to be in various metabolically highly active stages of their cell cycle. To induce cell cycle progression, normal T-cells were stimulated with a combination of 12-*O*-tetradecanoylphorbol-13-acetate (TPA) and ionomycin, while normal B-cells were stimulated through cross linkage of surface immunoglobulin. These cells were then probed for their Raman signatures to determine the extent to which the spectral differences between non-cancerous and cancer cells can be attributed to the differences in their metabolic activity associated with cell cycle progression. Figure 8 shows a comparison between the averaged Raman spectra of non-cancerous T and B cells in their resting (G0) and activated states. Figure 9 shows the position of the activated T and B cell groups relative to the normal and leukemia cell groups in a PCA plot. This plot shows that the activated cells fall within a region defined by the normal cells. The difference spectra between the activated T and B cells and their resting counterparts (Figure 8) indicate slight variations in the spectra, but their magnitude is much smaller than those observed between normal and leukemic cells. This data indicates that unique Raman markers exist that can discriminate cancer cells from both activated and resting normal cells.

What is the underlying cellular biology that accounts for the spectral differences between normal and cancer cells? Previous work (21,22) has suggested that these spectral differences are a reflection of cancerous cells being in different metabolic states than normal cells, which are predominantly in the G0 resting phase of their cell cycle. The decrease in local DNA concentration based on lower Raman intensities, in particular, has been attributed to higher levels of transcriptional and replicational activities occurring in metabolically more active cancer cells, which results in the decondensation of chromatin structure and an associated increase in proteins to support biomolecular synthesis. In addition, the morphology of cancer cells, specifically the enlarged nucleus, results in a lower DNA density in our probe volume. To evaluate this hypothesis, we compared the Raman spectra of cancer cells to those of

activated normal cells using PCA to determine the degree of overlap between the two cell types. Previous Raman measurements of T cell activation (15) have shown decreases in peak intensities at 785, 1093, 1376, and 1581 cm^{-1}, which are consistent with our data on activated normal cells. The spectral changes likely reflect alterations in the secondary or tertiary structure of nucleic acids, or an unfolding of the DNA molecules as the cells become more active in their transcription, leading to a locally lower DNA concentration as it expands and requires more space. In our PCA scatter plots, the cluster of activated normal cells is located in a separate region from the cancer cells and falls within the normal cell region. This suggests that the spectral differences between normal lymphocytes and leukemia cells are likely attributable to other factors that lead to more pronounced effects than just cell activation such as the faster proliferation rate of cancer cells, which results in more of the cells having heightened metabolic activity, cell growth differentiation, and transcriptional activity. Additional studies are currently in progress to more precisely control some of these aspects and further elucidate these issues.

Currently, a limitation of this technique is that only a small fraction of the entire cell can be analyzed due to the tightly focused beam that is required for optical trapping. As noted earlier, the remarkable reproducibility of our spectra for each cell type confirms that we are likely trapping an organelle with a high refractive index within the cell, i.e. the nucleus in our case. Although we have shown the ability to discriminate between normal and cancer cells based on spectral data acquired from this specific region of the cell, other parts of the cell may provide valuable spectral information that could improve the detection sensitivity. To capture a Raman spectrum that better represents the entire cell, modifications to the optical configuration of the laser trapping Raman method would be needed. An example is the use of a dual beam approach in which one beam is tightly focused to trap the cell while a second Raman excitation beam probes the Raman signature of the entire cell, either by rastering the beam across the cell or defocusing the beam to illuminate a larger fraction of the cell volume.

CONCLUSION

We have shown that Raman spectroscopy can probe the biochemical composition of individual cells with little to no major variations in the spectra due to different phenotypes or backgrounds of the human

subjects. Highly reproducible combinations of spectral markers that can be used to accurately classify normal and cancer cells have been identified. These markers, which indicate that the cancer cells exhibit a lower DNA to protein ratio than in normal cells, are consistent with our previous study using cultured cell lines. We also demonstrate the relatively subtle changes in the Raman spectra of cells due to cell activation or during different phases in the cell cycle, especially when compared to the differences between normal and cancer cells.

The realization that laser trapping Raman spectroscopy of single cells can accurately identify leukemia cells based on intrinsic optical signatures could lead to potential new approaches for cell sorting and analysis beyond the current capabilities of flow cytometry and other existing clinical methods for cancer diagnosis. These results are also particularly encouraging, because they provide evidence of the substantial potential that single cell Raman spectroscopy may have for the label-free analysis of not only cancer cells but also other cell types (e.g. stem cells) of interest in biomedicine. While the current rate at which single cells can be interrogated using spontaneous Raman spectroscopy is on the order of tens of seconds to several minutes, rapid progress in the area of coherent Raman spectroscopy and microscopy (23-25) to probe specific Raman bands at millisecond to microsecond timescales shows the potential for increasing the rate of analysis, bringing high-speed Raman cell sorting and screening within the reach of researchers and clinicians in the near future.

ACKNOWLEDGMENT

This work was supported by funding from the Laboratory Directed Research and Development Program at LLNL and was performed under the auspices of the U.S. Department of Energy by Lawrence Livermore National Laboratory in part under Contract W-7405-Eng-48 and in part under Contract DE-AC52-07NA27344 (for JC, SL). This work was supported by funding from the National Science Foundation. The Center for Biophotonics, an NSF Science and Technology Center, is managed by the University of California, Davis, under Cooperative Agreement No. PHY 0120999 (JC, DT, SL, TH). This work was also supported, in part, by grants from the Children's Miracle Network (DT), Keaton-Raphael Memorial Fund (DT), and a Technology Transfer Grant from the University of California, Davis (JC, DT). T.H. acknowledges support by the Clinical Translational Science Center under Grant Number UL1 RR024146 from the National Center for Research Resources (NCRR) a component of the National Institutes of Health (NIH), and NIH Roadmap for Medical Research. The authors gratefully thank Dr. Erica Chédin for reading the manuscript and providing fruitful suggestions.

FIGURE CAPTIONS

Figure 1. Mean Raman spectra of normal (a) T and (b) B cells from four healthy individuals. Each spectrum is an average of ~20 cells. All spectra exhibit similar, distinct Raman peaks that can be assigned to specific biochemical constituents (see text).

Figure 2. Averaged intensity values and standard deviations of select DNA peaks for normal (a) T and (b) B cell groups from different individuals. Calculated p-values for the 785, 1093, 1373 and 1575 cm^{-1} Raman peaks are as follows. For (a) 0.09, 0.85, 0.75, and 0.11. For (b) 0.06, 0.49, 0.63, and 0.08.

Figure 3. PCA scatter plots of normal (a) T and (b) B cells from four individuals using the first and second principal components. For both cell types, the four groups cluster together, indicating reproducibility of spectra from person to person.

Figure 4. Mean Raman spectra of normal and patient-derived leukemia cells. Comparisons are between (a) normal T – acute lymphoblastic leukemia (ALL) and (b), (c) two normal B – pre-B ALL cells. Also shown below the spectra are the difference spectra, obtained by subtracting the normal spectra from the cancer spectra, which show reproducible spectral differences in all three cases.

Figure 5. Comparison of the averaged intensity values and standard deviations of select DNA peaks for (a) normal and cancer T cells and (b) normal B and two pre-B cancer cells. The DNA Raman peak intensities of the cancer cells are noticeably lower. Calculated p-values for the 785, 1093, 1373, and 1575 cm-1 Raman peaks are as follows. For (a) $2.7x10^{-5}$, $3.4x10^{-3}$, $2.5x10^{-6}$, $2.3x10^{-5}$. For (b), $1.8x10^{-10}$, $3.4x10^{-11}$, $2.7x10^{-11}$, $6.2x10^{-5}$.

Figure 6. PCA scatter plots comparing (a) normal T and T-ALL and (b), (c) normal B and pre-B ALL cells based on the first and second PC. Two distinct groups form that separate normal from cancer cells. Shaded regions overlaid on the data points serve only as guides to the eye. A PCA-LDA classification routine estimates sensitivity levels to be comparable to flow cytometry results (see text).

Figure 7. Loading values plotted for each of the first principal components defined by the PCA scatter plots in figure 6. (a) (b) (c) Raman wavenumbers that have a large deviation from the zero baseline have a greater contribution to the principal component. These profiles are identical to the difference spectra in figure 3, which indicate that the differences in DNA and protein are indeed responsible for the separation in the PCA plots.

Figure 8. Mean Raman spectra comparing normal and activated (a) T and (b) B cells and their difference spectra. Each spectrum is an average of 15 cells. The spectral differences between the normal and activated cells are small in magnitude for both cell types, in particular when compared to the larger differences between normal and cancer cells (figure 3).

Figure 9. PCA plots illustrating the relative positions of normal, activated normal, and cancer cells for both (a) T and (b) B cells show that normal activated and normal resting cells cluster together and are indistinguishable. Shaded regions overlaid on the data points serve only as guides to the eye. This result suggests that the spectral signatures are unique cancer markers for leukemia.

TABLES

Table 1 – Raman spectral differences between normal and leukemic cells and their assignments

Raman frequency (cm^{-1})	Assignment
678	G (C-2'-endo-anti)
785	U, T, C, bk: O-P-O
1093	O-P-O sym. str., p: C-N
1126	p: C-N str.
1337	A, G, p: C-H def.
1373	T, A, G
1447	p: C-H_2 def.
1575	G, A
1605	Phe, Tyr, p: C=C
1615	Tyr, Trp, p: C=C
1650	p: amide I, l: C=C

*Abbreviations: def, deformation vibration, str, stretching, bk, vibration of the backbone, sym, symmetric, p, protein, U,C,T,A,G, ring breathing modes of DNA/RNA bases, Phe phenylalanine, Tyr tyrosine, Trp tryptophan, l lipid

REFERENCES

1. Haka, A. S., Volynskaya, Z., Gardecki, J. A., Nazemi, J., Lyons, J., Hicks, D., Fitzmaurice, M., Dasari, R. R., Crowe, J. P., and Feld, M. S. *Cancer Research* 2006, *66*, 3317-3322.

2. Shetty, G., Kendall, C., Shepherd, N., Stone, N., and Barr, H. *British Journal of Cancer* 2006, *94,* 1460-1464.

3. Krishna, C. M., Prathima, N. B., Malini, R., Vadhiraja, B. M., Bhatt, R. A., Fernandes, D. J., Kushtagi, P., Vidyasagar, M. S., and Kartha, V. B. *Vibrational Spectroscopy* 2006, *41,* 136-141.

4. Utzinger, U., Heintzelman, D. L., Mahadevan-Jansen, A., Malpica, A., Follen, M., and Richards-Kortum, R. *Applied Spectroscopy* 2001, *55,* 955-959.

5. Molckovsky, A., Song, L. M. W. K., Shim, M. G., Marcon, N. E., and Wilson, B. C. *Gastrointestinal Endoscopy* 2003, *57,* 396-402.

6. Xie, C. G., Li, Y. Q., Tang, W., and Newton, R. J. *Journal of Applied Physics* 2003, *94,* 6138-6142.

7. Xie, C. G., Dinno, M. A., and Li, Y. Q. *Optics Letters* 2002, *27,* 249-251.

8. Xie, C. G., Chen, D., and Li, Y. Q. *Optics Letters* 2005, *30,* 1800-1802.

9. Xie, C., Mace, J., Dinno, M. A., Li, Y. Q., Tang, W., Newton, R. J., and Gemperline, P. J. *Analytical Chemistry* 2005, *77,* 4390-4397.

10. Chan, J. W., Motton, D., Rutledge, J. C., Keim, N. L., and Huser, T. *Analytical Chemistry* 2005, *77,* 5870-5876.

11. Chan, J. W., Esposito, A. P., Talley, C. E., Hollars, C. W., Lane, S. M., and Huser, T. *Analytical Chemistry* 2004, *76,* 599-603.

12. Chan, J. W., Taylor, D. S., Zwerdling, T., Lane, S. M., Ihara, K., and Huser, T. *Biophysical Journal* 2006, *90,* 648-656.

13. Chen, K., Qin, Y. J., Zheng, F., Sun, M. H., and Shi, D. R. *Optics Letters* 2006, *31,* 2015-2017.

14. Chen, D., Huang, S. S., and Li, Y. Q. *Analytical Chemistry* 2006, *78,* 6936-6941.

15. Mannie, M. D., McConnell, T. J., Xie, C. G., and Li, Y. Q. *Journal of Immunological Methods* 2005, *297,* 53-60.

16. Deng, J. L., Wei, Q., Zhang, M. H., Wang, Y. Z., and Li, Y. Q. *Journal of Raman Spectroscopy* 2005, *36,* 257-261.

17. Singh, G. P., Creely, C. M., Volpe, G., Grotsch, H., and Petrov, D. *Analytical Chemistry* 2005, *77,* 2564-2568.

18. Singh, G. P., Volpe, G., Creely, C. M., Grotsch, H., Geli, I. M., and Petrov, D. *Journal of Raman Spectroscopy* 2006, *37,* 858-864.

19. Lieber, C. A. and Mahadevan-Jansen, A. *Applied Spectroscopy* 2003, *57,* 1363-1367.

20. Notingher, L., Jell, G., Notingher, P. L., Bisson, I., Tsigkou, O., Polak, J. M., Stevens, M. M., and Hench, L. L. *Journal of Molecular Structure* 2005, *744,* 179-185.

21. Uzunbajakava, N., Lenferink, A., Kraan, Y., Willekens, B., Vrensen, G., Greve, J., and Otto, C. *Biopolymers* 2003, *72,* 1-9.

22. Notingher, I., Jell, G., Lohbauer, U., Salih, V., and Hench, L. L. *Journal of Cellular Biochemistry* 2004, *92,* 1180-1192.

23. Chan, J. W., Winhold, H., Lane, S. M., and Huser, T. *IEEE Journal of Selected Topics in Quantum Electronics* 2005*, 11,* 858-863.

24. Cheng, J. X. and Xie, X. S. *Journal of Physical Chemistry B* 2004, *108,* 827-840.

25. Ploetz, E., Laimgruber, S., Berner, S., Zinth, W., and Gilch, P. *Applied Physics B-Lasers and Optics* 2007, *87,* 389-393.

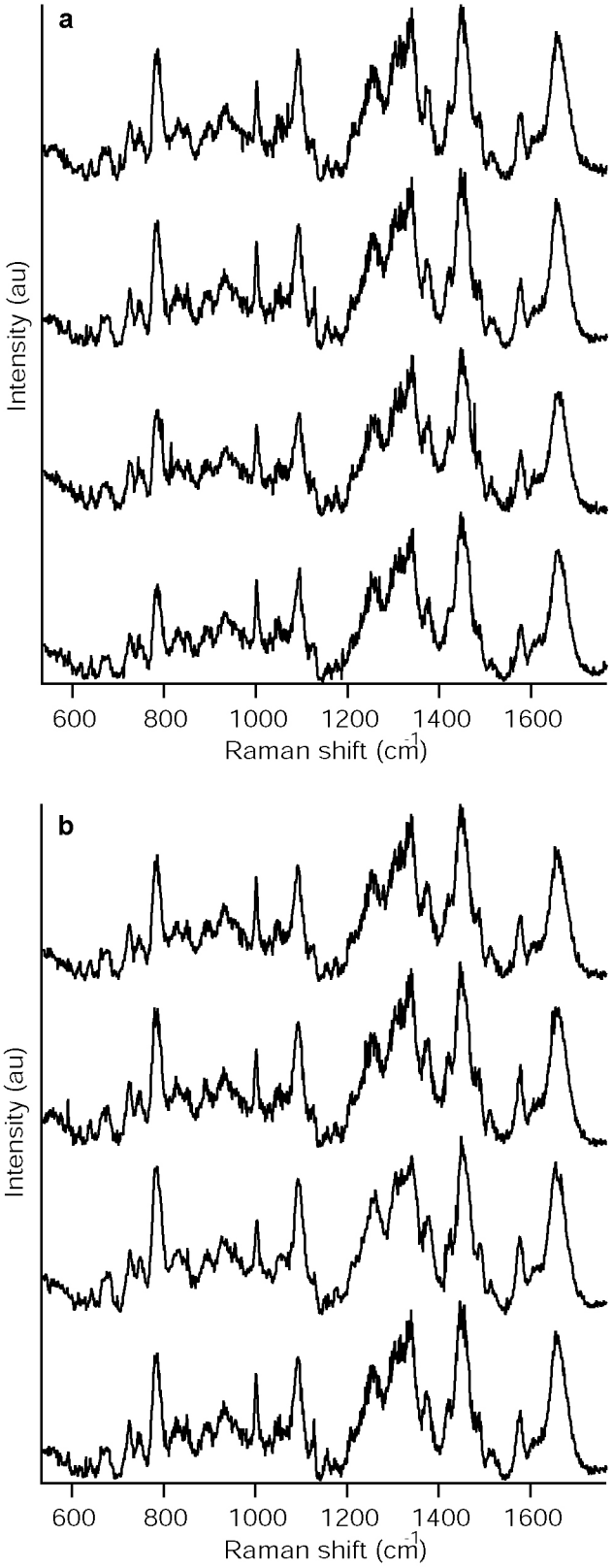

Figure 1. Chan et. al.

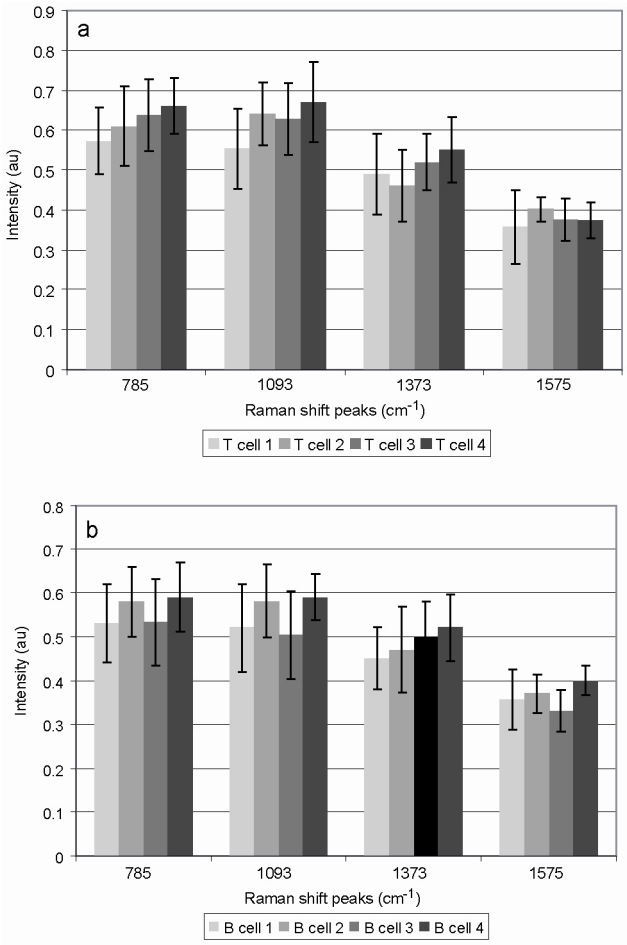

Figure 2. Chan et. al.

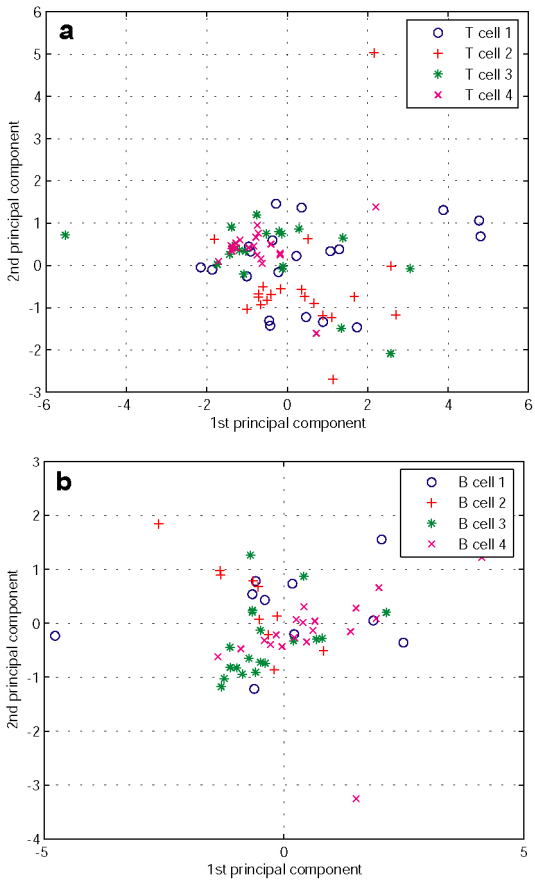

Figure 3. Chan et. al.

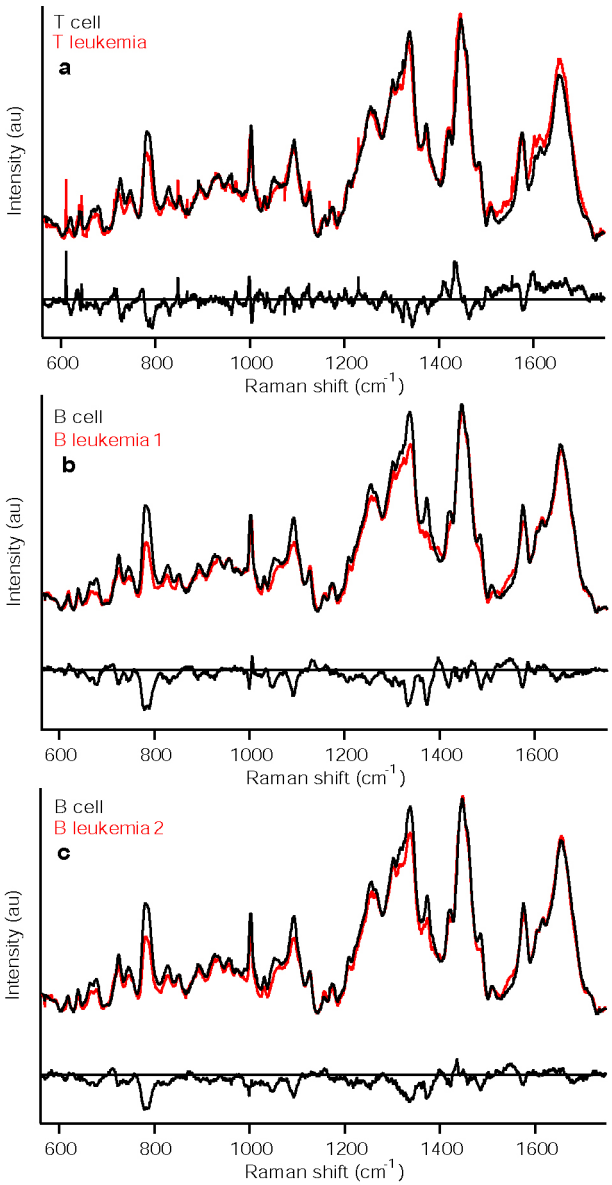

Figure 4. Chan et. al.

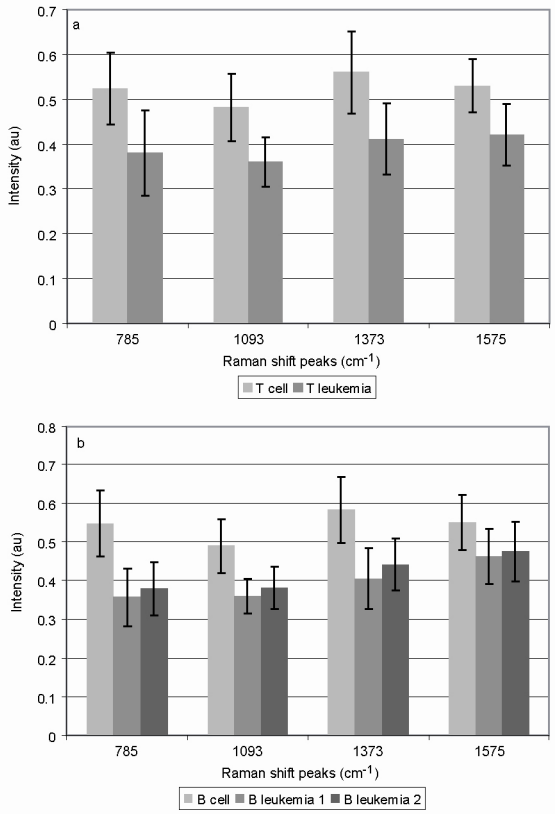

Figure 5. Chan et. al.

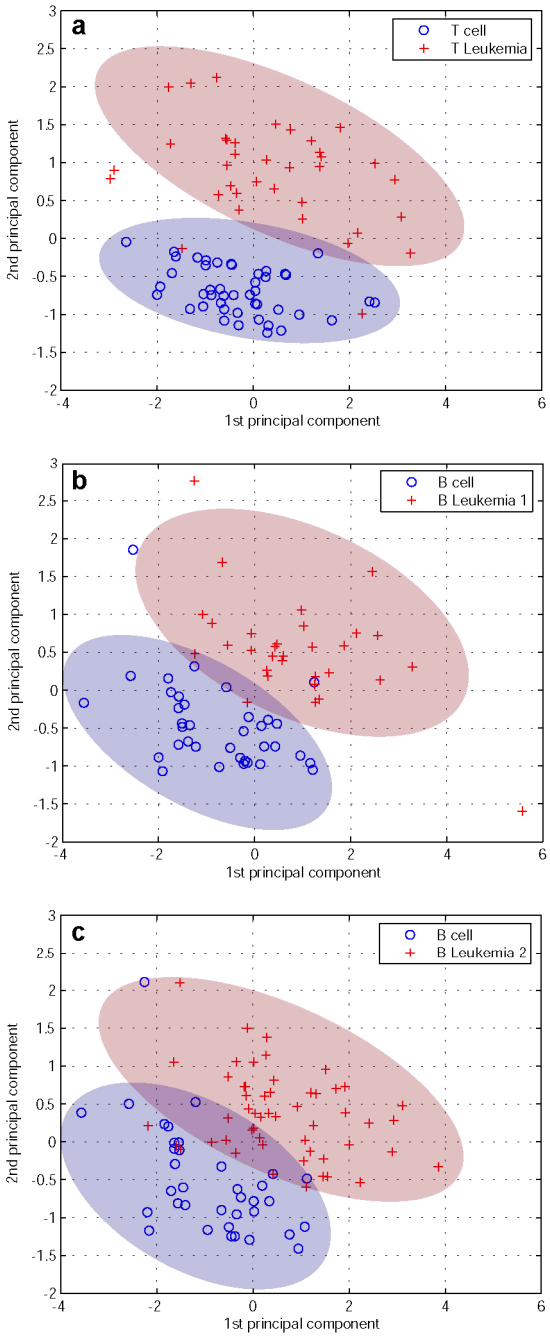

Figure 6. Chan et. al.

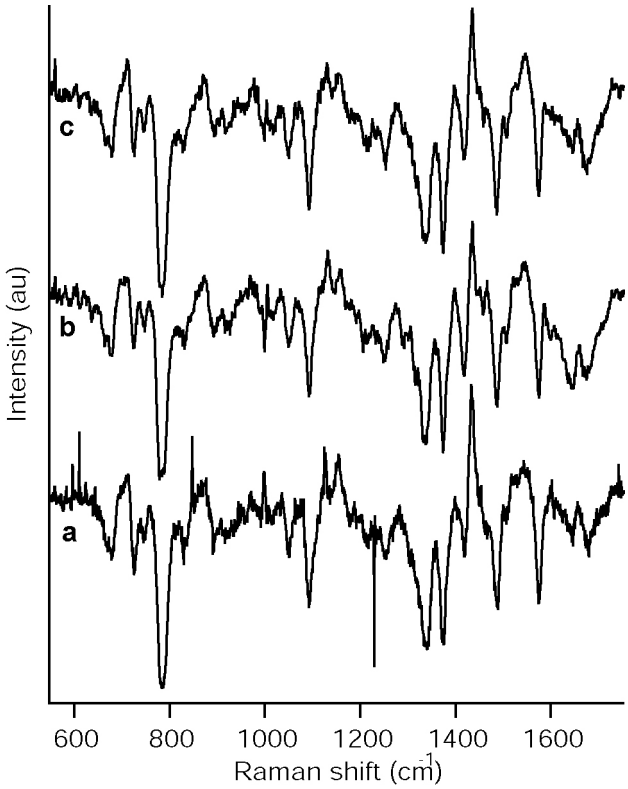

Figure 7. Chan et. al.

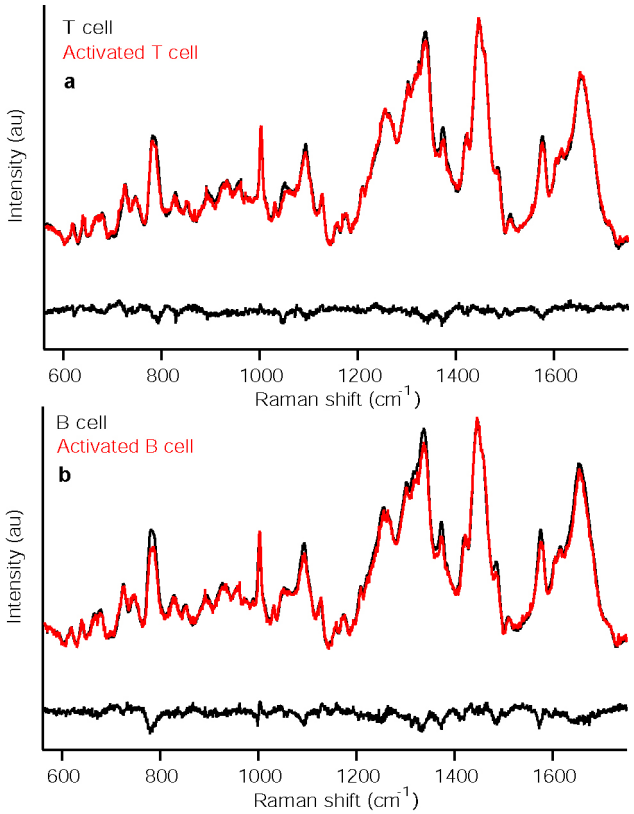

Figure 8. Chan et. al.

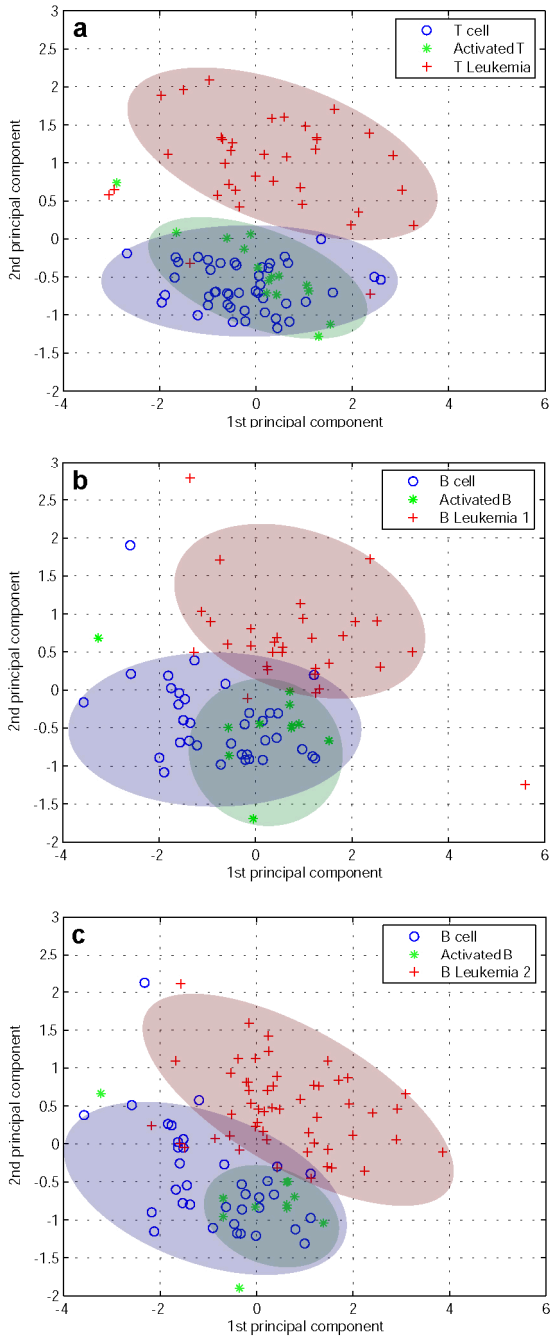

Figure 9. Chan et. al.